Soil Dynamics and Earthquake Engineering 57 (2014) 152–163

Contents lists available at ScienceDirect

Soil Dynamics and Earthquake Engineering

journal homepage: www.elsevier.com/locate/soildyn

Requirements for soil-specific correlation between shear wave velocity and liquefaction resistance of sands

Mohammad Mehdi Ahmadi*, Nima Akbari Paydar

Department of Civil Engineering, Sharif University of Technology, P.O. Box 11365-11155, Azadi Avenue, Tehran, Iran

ARTICLE INFO

Article history:
Received 30 January 2013
Received in revised form
11 July 2013
Accepted 7 November 2013
Available online 14 December 2013

Keywords:
Liquefaction resistance
Shear wave velocity
Cyclic triaxial test
Bender element test

ABSTRACT

The application of the simplified method for evaluating the liquefaction potential based on shear wave velocity measurements has increased substantially due to its advantages, especially for microzonation of liquefaction potential. In the simplified method, a curve is proposed to correlate the cyclic resistance ratio (CRR) with overburden stress-corrected shear wave velocity (V_{s1}). However, the uniqueness of this curve for all types of soils is questionable. The objective of this research is to study whether the correlation between CRR and V_{s1} is unique or not. Besides, the necessity of developing the soil-specific correlations is also investigated. Based on laboratory test data, a new semi-empirical method is proposed to establish the soil-specific CRR–V_{s1} correlation. To validate the proposed method, a number of undrained cyclic triaxial tests along with bender element tests were performed on two types of sands. Similar experimental data for six other types of sands reported in the literature was also compiled. Applying the proposed method, soil-specific CRR–V_{s1} correlation curves were developed for these eight types of sands. It is shown that the correlation is not unique for different types of sands and the boundary curve proposed in the available simplified method can only be used as an initial estimation of liquefaction resistance. Finally, using the results of this study as well as previous ones, a chart is suggested to be used in engineering practice showing the conditions for which a detailed soil-specific CRR–V_{s1} correlation study needs to be performed.

1. Introduction

Evaluation of seismic liquefaction potential of soils is an important and challenging issue in geotechnical earthquake engineering. The simplified method, initially developed by Seed and Idriss [1], has been used in engineering practice and evolved as a standard method in the liquefaction resistance evaluation. In this method, based on standard penetration test (SPT), cone penetration test (CPT), or shear wave velocity (V_s) measurements, a boundary curve is proposed to separate the liquefiable and non-liquefiable soil zones.

To evaluate liquefaction resistance of sandy soils, V_s measurements offer geotechnical engineers a promising alternative and a supplementary tool compared to penetration-based methods, such as SPT and CPT [2]. Many parameters can affect the V_s of a soil, among which effective confining stress, void ratio, stress history, grain characteristics, aging effects and soil structure can be mentioned as the most important. These parameters can also affect the liquefaction resistance of soils [3,4]. Considering this fact, the idea of using V_s to evaluate the liquefaction resistance of soils has received considerable attention. De Alba et al. [5] were among the first researchers who proposed the correlation between V_s and liquefaction resistance (CRR–V_s curve). CRR stands for cyclic resistance ratio which is defined as the cyclic liquefaction resistance normalized by initial overburden effective stress.

The advantages of using shear wave velocity for evaluation of liquefaction potential, compared to penetration-based methods, are as follows:

- V_s can be measured in soils, such as gravelly soils, that are hard to sample. In these types of soils penetration tests may be unreliable [2,4].
- V_s is one of the few parameters that are measurable both in the laboratory and in the field. If a relationship is obtained for shear wave velocity in the laboratory, it can also be used on site [4].
- There is no need for drilling boreholes in this method, and it can predict the liquefaction resistance more rapidly and economically than SPT or CPT; therefore, it can be used in microzonation of liquefaction potential [2,4].
- The cyclic resistances of intact and reconstituted samples are quite different [6]. However, if a reconstituted sample is

* Corresponding author. Tel.: +98 21 66164220; fax: +98 21 66014828.
E-mail address: mmahmadi@sharif.edu (M.M. Ahmadi).

0267-7261/$ - see front matter © 2013 Elsevier Ltd. All rights reserved.
http://dx.doi.org/10.1016/j.soildyn.2013.11.001

Nomenclature

a, b	curve fitting parameters for the data presented by Andrus and Stoke
C_c	coefficient of curvature
C_g, a_g, n_g	intrinsic soil parameters in the small-strain shear modulus evaluation from e and σ'_m
CRR	cyclic liquefaction resistance ratio
$CRR_{tx\text{-}15\ cycles}$	liquefaction resistance ratio from triaxial test
CSR	cyclic stress ratio
CSR_{M_w}	cyclic stress ratio for an earthquake magnitude of M_w
CSR_{tx}	cyclic shear stress ratio from triaxial test
C_u	coefficient of uniformity
D_{50}	mean grain size
DA	double amplitude axial strain
e	void ratio
e_{max}	maximum void ratio
e_{min}	minimum void ratio
G_0	small-strain shear modulus
G_{01}	field small-strain shear modulus at a vertical effective stress of 100 kPa
$G_{01,\ tx}$	laboratory small-strain shear modulus at an effective confining stress of 100 kPa
G_s	specific gravity of solids
K_0	coefficient of lateral earth pressure at rest
K_c, n_c	proposed CRR–V_{s1} field correlation coefficients
L	tip-to-tip distance of bender elements
MSF	earthquake magnitude scaling factor
M_w	earthquake magnitude
P_A	reference stress (=100 kPa)
q	deviatoric stress
R^2	correlation coefficient
t	travel time of the wave in bender element tests
V^*_{s1}	limiting upper value of V_{s1} for cyclic liquefaction occurrence by the Andrus and Stoke method
V_s	shear wave velocity
$V_{s,\ field}$	in situ measured shear wave velocity
V_{s1}	field overburden stress normalized shear wave velocity
$V_{s1,\ tx}$	normalized shear wave velocity to confining stress of 100 kPa
α	coefficient in Eq. (2) to correlate cyclic liquefaction resistance ratio and void ratio
β	a power in Eq. (2) to correlate cyclic liquefaction resistance ratio and void ratio
$\Delta\sigma_d$	cyclic deviator stress
ρ	total density
σ'_{c0}	initial effective confining stress
σ'_m	mean effective stress
σ'_v	vertical effective stress

prepared to the same V_s as an intact sample, then the liquefaction resistance of both samples is equal; In other words, the reconstituted samples can be used to establish the correlation between V_s and CRR [3,7]. This issue is expected to be valid for uncemented Holocene-age soils (< 10,000 years) or freshly deposited soils. For older deposits, its validity is open to question and aging factor may need to be used [8].

- The correlation between V_s and CRR is independent of the stress history of the soil as well as the method used to prepare the sample for cyclic testing [3].
- V_s is a significant soil property in earthquake site response and soil-structure interaction analyses. It has a clear physical meaning, whereas the penetration resistance cannot directly correspond to any of such properties [4].

Use of V_s to evaluate the liquefaction potential has some limitations. These include:

- No samples are routinely obtained as part of the testing procedure for soil classification and identification of non-liquefiable materials [2].
- Thin, low V_s liquefiable strata may not be detected if the measurement interval is too large [9,10].
- V_s measurements are made at small-strains, whereas pore water pressure buildup and liquefaction are medium to high-strain phenomena [11]. This can be a significant disadvantage for cemented soils. This is because small-strain measurements are highly sensitive to weak inter-particle bonds that are eliminated at medium to high strains. It can also be significant in silty soils above the water table where negative pore water pressures may increase the shear wave velocity [2].
- V_s may not be expected to reflect the critical friction angle and dilatancy of the soil, both of which are known to affect liquefaction resistance [12]. Critical friction angle and dilation increase with increasing non-plastic fines, whereas the shear wave velocity decreases [13].
- The different methods of measuring/estimating V_s sample different volumes of soil (e.g. SASW, MASW, CPT–V, cross-hole, and suspension logger) and it can be difficult to compare laboratory and field data.

Besides these disadvantages, it should also be noted that both V_s and CRR are affected by soil type, and therefore, the correlation of these two parameters may also be affected by soil type. Based on database of various sandy soils, different CRR–V_s correlations have been proposed by different researchers [2,4,14–19]. Therefore, one of the major challenges associated with the use of V_s to evaluate the liquefaction resistance, is the uniqueness of V_s–CRR correlation for all sands.

Tokimatsu and Uchida [4] showed that the correlation between small-strain shear modulus, G_0, and CRR (and consequently between V_s and CRR) are different for two types of sand, Niigata sand and Toyoura sand (Fig. 1(a)). Their attempt to provide unique curve for different sands, has led to curve (b) in Fig. 1. In this curve, the effect of sand type is intended by $F(e_{min})$ which is a function of the minimum void ratio ($F(e_{min})=(2.17-e_{min})^2/(1+e_{min})$). This is also indicative of the correlation dependence on sand type. This argument is reinforced because recent studies also have shown that CRR–V_s correlation is soil-specific [3,19,20]. On the other hand, the simplified and widely used field based procedure of Andrus and Stokoe [2] recommended by NCCER is considered to be independent of soil type. However, the relationship proposed by Andrus and Stokoe [2] which is presented in detail in Section 7.2, is highly based on limiting upper value of V_s for cyclic liquefaction occurrence. Since cyclic stress ratio (CSR) values above about 0.35 are limited in the case history data gathered by Andrus and Stokoe, current estimates of upper values of V_s rely on penetration–V_s correlations [2]. However many penetration–V_s correlations have been proposed so far for different sandy soils. If these different correlations are used, different values for upper value of V_s will be obtained which in turn, result in different curves for CRR–V_s correlations. It means that the CRR–V_s correlation suggested by Andrus and Stokoe [2] also depends on the soil type and therefore, the CRR–V_s correlation may not be unique. Due to these contradictions and ambiguities, one of the aims of this study is to clarify whether the correlation between CRR and V_s is unique or not. Also, the reliability

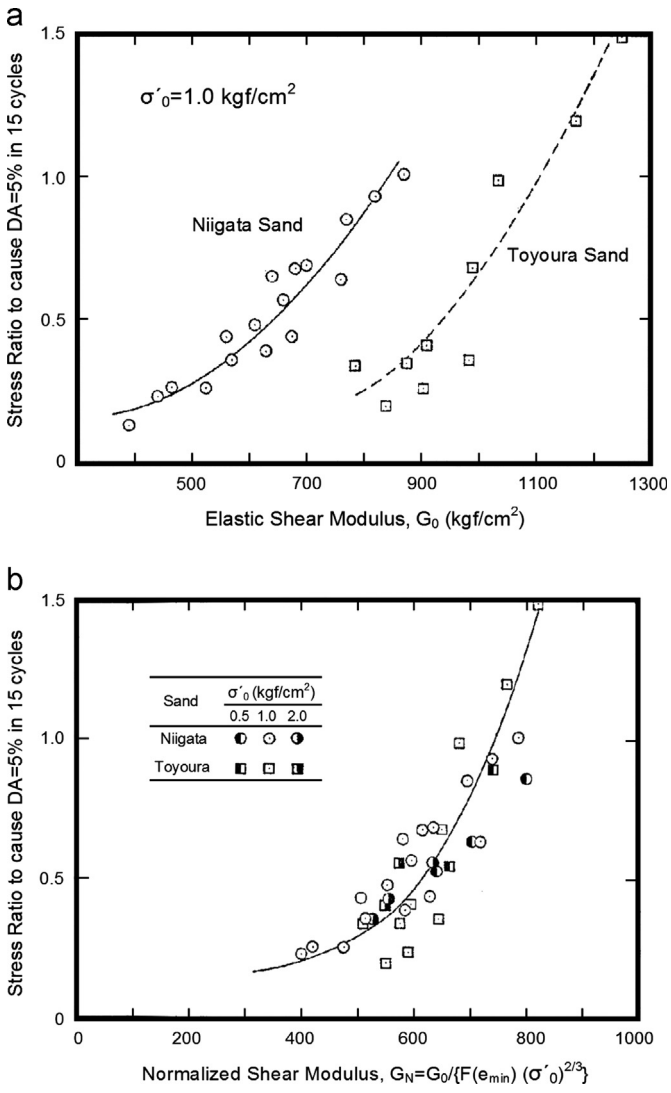

Fig. 1. Liquefaction resistance against (a) shear modulus and (b) normalized shear modulus for two sands [4].

and accuracy of the existing CRR–V_s correlations is investigated in this study.

Besides, previous studies have shown that, development of soil-specific correlations from laboratory tests may be costly and time-consuming [3,19,20]. Therefore, another objective of this study is to investigate the necessity of developing the soil-specific correlations.

In this study, based on laboratory data, a new semi-empirical method is proposed to develop a soil-specific correlation between CRR and V_s. Two types of sands were tested, and correlations are established based on the experimental results: one is a beach sand from the city of Babolsar, Iran (called Babolsar sand) and the other is a crushed silica sand from Firoozkooh mine (called Firoozkooh sand). Besides, similar experimental data for six other sands were also collected and compiled from previously published literature. Using the proposed method, the soil-specific correlation between liquefaction resistance and V_s are developed for each of these sand types.

Obtained correlations for different sand types using the suggested method in this study are compared with the method of Andrus and Stokoe [2] and other similar previously proposed methods. Finally, the uniqueness of the CRR–V_s correlation and the necessary conditions for which a detailed soil-specific CRR–V_{s1} correlation study is needed, especially for microzonations of liquefaction potential, are discussed by using the laboratory based as well as field performance results.

2. Method for establishing CRR–V_s correlation

Many studies have been conducted to correlate the V_s with liquefaction resistance of sands based on general format of the Seed–Idriss simplified procedure [1]. This simplified procedure is the introduction of an empirical correlation to evaluate the cyclic resistance ratio (CRR) from field test results (e.g. N from SPT, q_c from CPT, or V_s). Following this simplified procedure; various methods for evaluation of the seismic liquefaction potential of soils from V_s measurement have been developed. These include:

- Methods based on a combination of laboratory measurement of V_s and liquefaction resistance [4,5,7,18,19,21,22].
- Methods based on in-situ measurements of V_s and an appropriate correlation between liquefaction resistance and V_s (i.e. field performance observations) [2,15,16,23,24]. Most of the in-situ shear wave measurements used in this method are post earthquake properties, and do not exactly reflect the initial state of the soil before earthquake [19]. On the other hand, liquefaction can only be judged from surface observations such as sand boils, or large settlements. Factors such as the existence of a superficial non-liquefiable thick layer would prevent the appearance of these surface indications. Also local information from sites that have been liquefied previously and the shear wave velocities have been measured on them before the occurrence of liquefaction is very limited. Conditions such as the lack of information about the type and percentage of fine materials, and the lack of awareness about whether the soil layer is fully saturated or not, can also severely affect this local information. Therefore, these in-situ V_s-based methods are still less well defined [10,16].
- Methods based on analytical investigations [25].
- Methods based on penetration–V_s correlations [17].
- Probability-based methods using statistical analysis [26,27]. These methods are applied to the results of the other above four methods.

Because of the more accurate and well-controlled conditions of laboratory methods, this method is used in this study to develop the CRR–V_s correlation. For this purpose, laboratory measurements of V_s using bender elements and liquefaction resistance estimations using cyclic triaxial tests were performed.

In order to develop a correlation between liquefaction resistance and V_s from experimental data (CRR–V_s relationship), a soil-specific relationship between liquefaction resistance and void ratio (e) is proposed (CRR–e relationship). The small-strain shear modulus (G_0) can be calculated from measured V_s (G_0–V_s relationship). Also, G_0 is related to the void ratio through the existing empirical soil-specific relationships (G_0–e relationship). Eliminating the void ratio between CRR–e and G_0–e relationships and using G_0–V_s relationship, the liquefaction resistance is correlated with V_s and hence, a new CRR–V_s relationship is developed. This method has been verified by using the data obtained from sands tested in this study and was used for experimental data collected for six other types of sands from previous studies. Using the proposed method, the soil-specific CRR–V_s correlations for these eight different types of sands are developed.

3. Tested materials

Two types of clean sands were used in this study. The first was Babolsar sand, a beach sand from north of Iran with sub-rounded grains. The second one was Firoozkooh no. 161 crushed silica sand with angular grains. Firoozkooh sand is a commercially available material from Firoozkooh mine in north-east of Tehran. The scanning electron microscope (SEM) images in Fig. 2 show different grain shapes of these two sands.

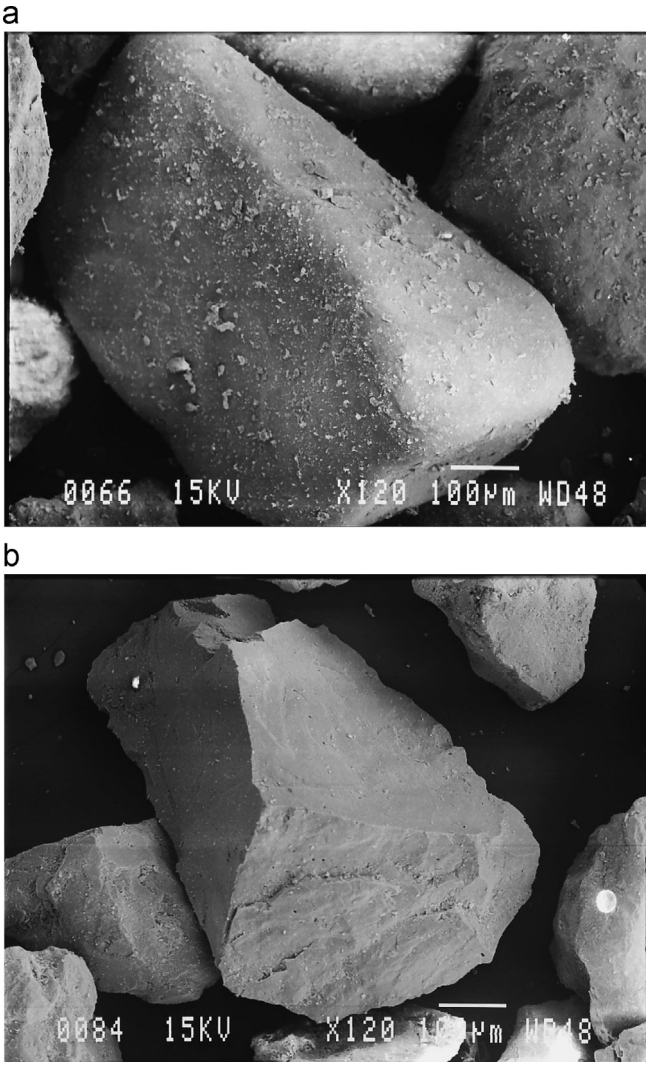

Fig. 2. Scanning electron microscope (SEM) image of (a) Babolsar sand and (b) Firoozkooh sand.

Table 1
Physical properties of tested sands.

Sand type	D_{50}	C_u	C_c	e_{max}	e_{min}	G_s
Babolsar	0.24	1.80	1.00	0.825	0.546	2.78
Firoozkooh	0.23	1.32	0.92	0.886	0.637	2.65

Both sands are used as standard sands in geotechnical testing in Iran. A summary of the physical properties of these sands is given in Table 1, and the corresponding grain size distribution curves are shown in Fig. 3. These sands have nearly identical particle size distributions. ASTM D 4253 and ASTM D 4254 standard test methods were used to determine the minimum and maximum void ratios, respectively.

4. Cyclic triaxial testing

The cyclic resistance of the sands tested was determined using undrained stress-controlled cyclic triaxial tests performed on reconstituted specimens. The tested specimens were 70 mm in diameter and 140 mm in height. In order to measure the V_s and liquefaction resistance on a single sample, the bender elements were assembled

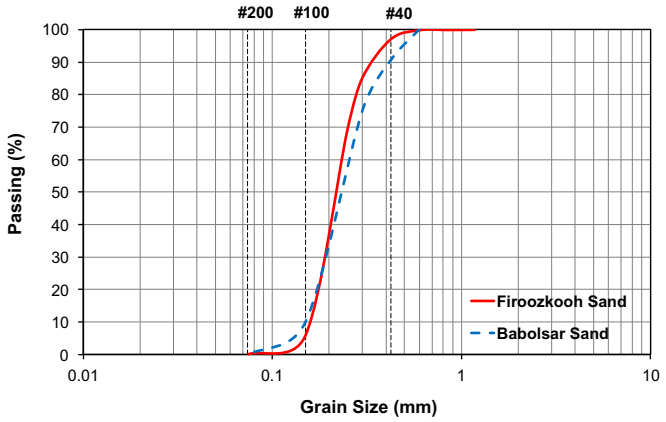

Fig. 3. Grain size distributions of tested sands.

on the cyclic triaxial apparatus. These bender elements were installed at the top and bottom pedestal of the triaxial cell. The cyclic triaxial apparatus used in this testing program is manufactured by Wykeham Farrance England, Ltd. Furthermore, some modifications were made to this apparatus. This apparatus is a digitally controlled, servo-pneumatic, closed-loop system, which controls three parameters: axial stress, confining pressure, and back pressure. A diagram of the automated triaxial system equipped with bender elements is shown schematically in Fig. 4.

4.1. Specimen preparation

Tokimatsu and Uchida [4] and also Huang et al. [22] argued that specimen preparation method does not affect the liquefaction resistance–V_s correlations. Among the different kinds of specimen reconstitution methods, the moist tamping method gives the widest range of void ratios [28]. Huang et al. [22] showed that the specimens prepared by moist tamping are reasonably uniform and give sufficiently repeatable V_s values. Therefore, moist tamping method of sample reconstitution with 5% water content was used to homogeneously prepare the samples. In order to obtain a uniform density, the specimens were made in seven layers and the under-compaction method, proposed by Ladd [29], was used.

4.2. Testing procedure

ASTM D 5311 standard testing procedure for load controlled cyclic triaxial strength of soil was used to conduct the experiments.

To facilitate the saturation process, carbon dioxide (CO_2) was first passed through the samples. Subsequently deaired water was allowed to flow in the specimens. Samples were then saturated by applying proper back pressure in successive steps. The Skempton pore pressure parameter (B) was determined as a means of degree of saturation. According to ASTM D 5311, samples are considered to be fully saturated if B value is at least equal to or greater than 0.95. Saturated samples were then consistently consolidated uniformly in steps of 10–30 kPa. The consolidation process continued until the effective confining stress reached a value of 200 kPa. Since increasing the consolidation stress can improve the vertical load controlling in the triaxial apparatus (Fig. 5), a consolidation stress of 200 kPa was chosen to perform the cyclic triaxial tests. Also, as is mentioned in Section 5.1, by increasing the consolidation stress, more bender elements tests can be conducted. Thus, possible errors are decreased and accuracy of the results is increased. On the other hand, Boulanger [30] pointed out that confining stress will be critical only for liquefaction evaluations at high overburden stresses. Therefore, liquefaction resistance of samples at consolidation stress of 100 or 200 KPa would not be much different.

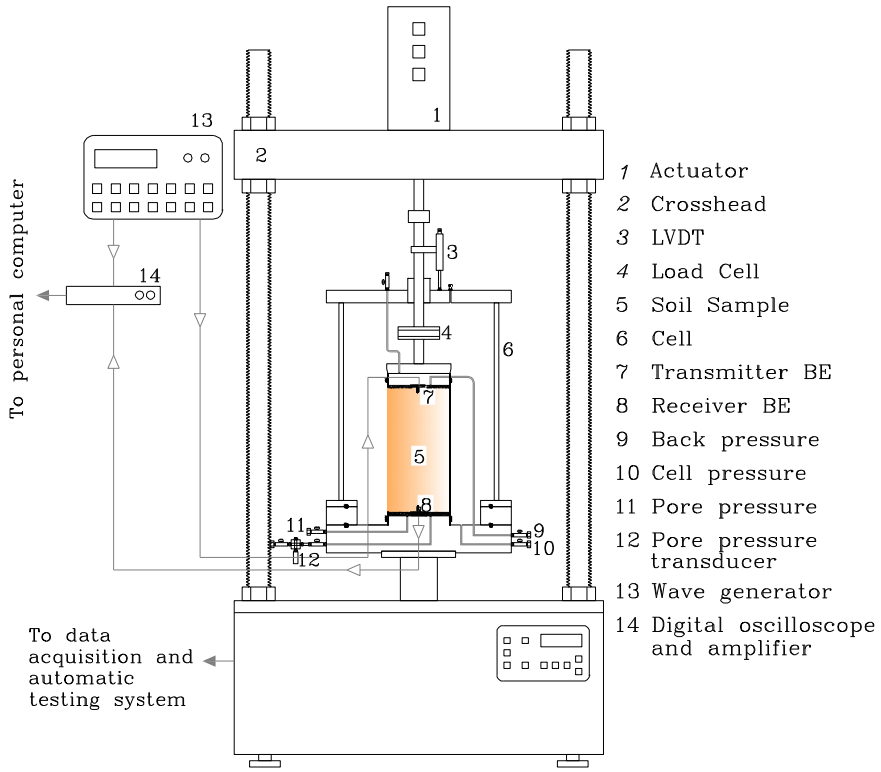

Fig. 4. Schematic diagram of the triaxial system equipped with bender elements.

At the end of consolidation process, a sinusoidal loading of 1 Hz frequency was applied to the sample having a specified cyclic shear stress ratio (CSR_{tx}). CSR_{tx} is defined as:

$$CSR_{tx} = \frac{\Delta\sigma_d}{2\sigma'_{c0}} \quad (1)$$

where $\Delta\sigma_d$ is the maximum cyclic deviator stress; and σ'_{c0} is the initial effective confining stress.

For each test, the number of cycles required for the initial liquefaction of the sample, when pore water pressure firstly reaches the initial consolidation stress, has been recorded. Cyclic resistance ratio in triaxial tests ($CRR_{tx\text{-}15\ cycles}$) is defined as the applied CSR_{tx} required to cause initial liquefaction in 15 cycles of loading (representing an earthquake magnitude of $M_w = 7.5$). At least three cyclic triaxial tests were performed to obtain $CRR_{tx\text{-}15\ cycles}$ for a soil sample having a specified void ratio. All parameters except CSR_{tx} were kept constant in these tests.

The after consolidation void ratio of the samples was determined by accurately measuring the water content of the entire sample at the end of the experiment when the cyclic loading has been applied. To measure the water content of the sample, at the first step, the bottom valve of the sample was opened and a confining stress of approximately 50 kPa was applied. The free water weight, expelled from the sandy sample, was accurately measured. At the second step, the entire moist sample was carefully taken out of the apparatus and its moisture content was also measured. The water content of the sample is the sum of the free water measured in the first step and the moist content measured in the second step.

4.3. Test result

Sample records of a cyclic triaxial test on Firoozkooh sand with a void ratio of $e = 0.77$ and cyclic stress ratio of $CSR_{tx} = 0.231$ are presented in Fig. 5. In this figure, cyclic deviatoric stress, excess pore pressure ratio, and axial strain are all plotted against the number of loading cycles. The effective stress path for the test is also plotted in this figure. For this test, the specimen reached its initial liquefaction at the 39th cycle.

Tests results, in the form of CSR_{tx} versus the number of cycles for different void ratios, are shown in Fig. 6. As expected, the liquefaction resistance decreases as the void ratio increases.

It is worth noting that in Fig. 6(b), the single point specified by a dotted circle corresponds to the results previously presented test in Fig. 5. According to Fig. 6(b), the liquefaction resistance of Firoozkooh sand with a void ratio of $e = 0.77$ is equal to $CRR_{tx\text{-}15\ cycles} = 0.255$. The same way, the liquefaction resistance of a soil at different void ratios can be obtained from the results of the conducted tests presented in Fig. 6. If the liquefaction resistance ($CRR_{tx\text{-}15\ cycles}$) versus void ratio is plotted, a power curve with the following expression (Eq. (2)) can be fitted to the data points of different sand types. This is shown in Fig. 7 indicating that for identical void ratios, the liquefaction resistances of both tested sands are almost the same.

$$CRR_{tx-15\ cycles} = \alpha e^{\beta} \quad (2)$$

where e is the void ratio, and α and β are constants for a given material in a specified test conditions.

According to Fig. 7, $\alpha = 0.101$, $\beta = -3.618$ and $\alpha = 0.0897$, and $\beta = -3.799$ yield the best fit curves for Babolsar and Firoozkooh sands, respectively. The values of correlation coefficient, R^2, for both sand types are very close to 1.0, indicating that the correlation is satisfactory and Eq. (2) works well.

5. Bender element tests

Conducting an experiment with bender elements, V_s can be calculated using Eq. (3). In this equation, L is the distance between two bender elements and t is the travel time which is determined by recording the input and output voltages.

$$V_s = L/t \quad (3)$$

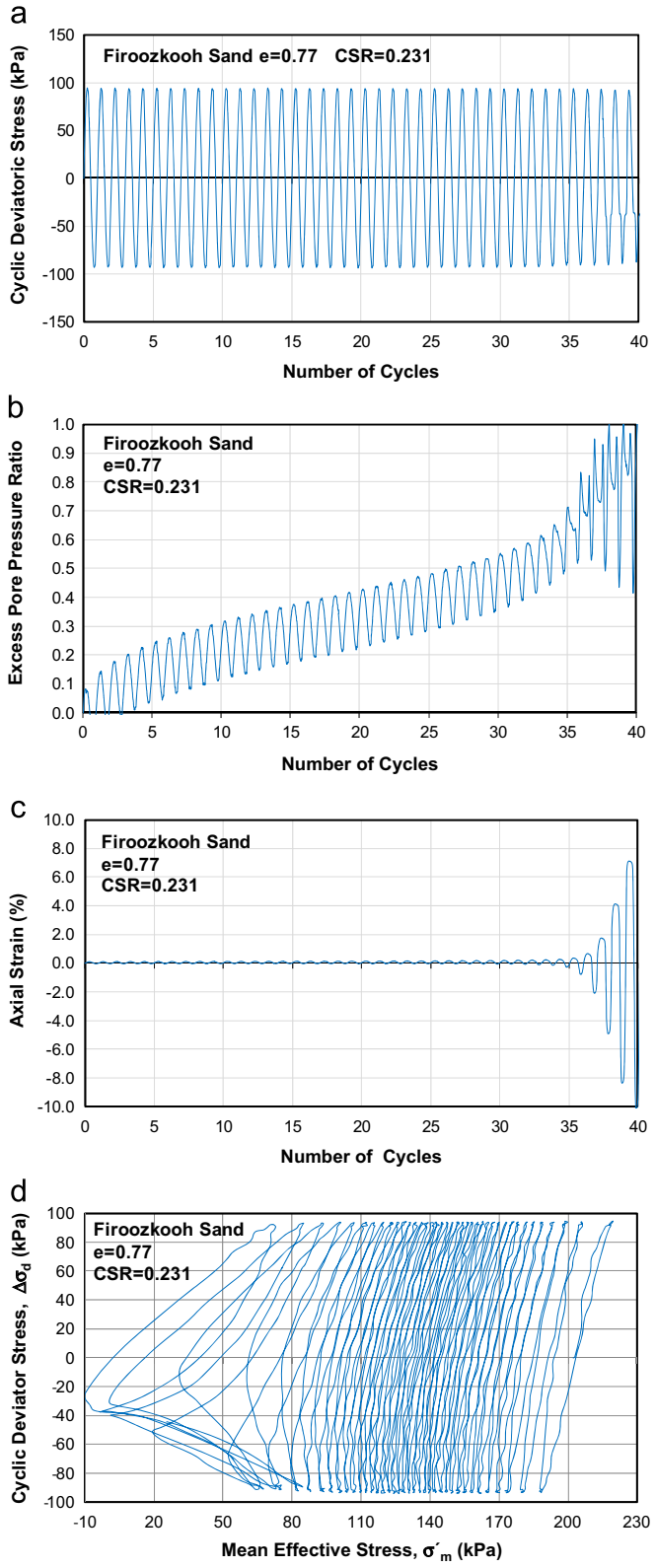

Fig. 5. Representative results of cyclic triaxial tests.

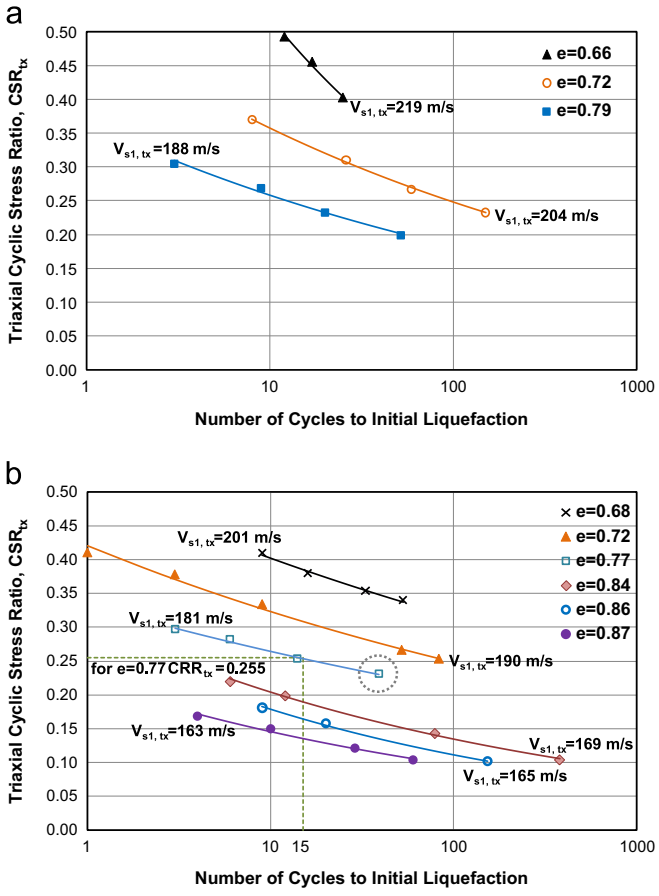

Fig. 6. Triaxial liquefaction curves of (a) Babolsar sand and (b) Firoozkooh sand.

5.1. *Testing procedure*

In the bender element tests performed in this study, a single sinusoidal pulse having a frequency of 5 kHz was used as the transmitted signal. The value of L in Eq. (3) is the tip-to-tip distance of the bender elements [31]. The method of first arrival time was used to obtain the travel time from source to receiver. In this method, the initial portion of the weak signal is ignored, and the time interval between the start of the source signal and the start of the major cycle of the received signal is measured. This weak signal indicates the presence of the near field effect, and should be eliminated [31,32].

For each sample, prior to the application of the cyclic loading, shear wave velocities were measured immediately after the end of each consolidation step for confining effective stresses ranging from 30 to 200 kPa.

Sample result of a bender element test on Babolsar sand with a void ratio of 0.806 at an effective confining stress of 70 kPa is represented in Fig. 8 in which the first arrival time is shown.

The void ratio as well as the height of the samples changes in each consolidation step as the confining stress increases. To calculate the changes in the void ratio, the amount of water expelled from the specimen during consolidation stage was measured using a sensitive volume change apparatus. Also, as mentioned in Section 4.2, the water content of the entire sample was carefully measured at the end of the experiment. Given that the sample is saturated prior to the consolidation phase, the void ratios at the earlier steps of consolidation can be back-calculated from these measured values. The settlement of the sample was also measured during the saturation and consolidation phase using a displacement transducer, and the change in the height of the samples was accordingly used in calculating the shear wave velocity using Eq. (3). An example of the results obtained for a single sample is presented in Fig. 9.

In this research, a total number of 350 bender element tests were carried out on 35 different samples of two sands, and a series of void ratio, confining effective stress, and V_s data were obtained

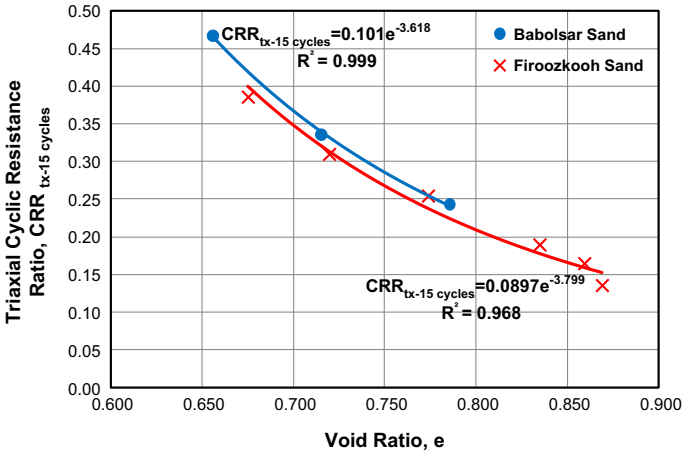

Fig. 7. Laboratory liquefaction resistance against void ratio for tested sands.

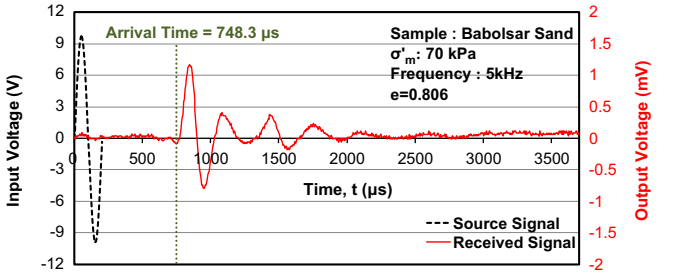

Fig. 8. Representative result of bender element tests.

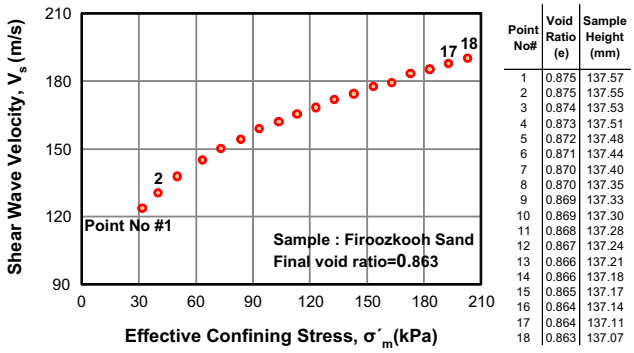

Point No#	Void Ratio (e)	Sample Height (mm)
1	0.875	137.57
2	0.875	137.55
3	0.874	137.53
4	0.873	137.51
5	0.872	137.48
6	0.871	137.44
7	0.870	137.40
8	0.870	137.35
9	0.869	137.33
10	0.869	137.30
11	0.868	137.28
12	0.867	137.24
13	0.866	137.21
14	0.866	137.18
15	0.865	137.17
16	0.864	137.14
17	0.864	137.11
18	0.863	137.07

Fig. 9. An example of shear wave velocity measurement at different steps of consolidation.

for each type of sands. Fig. 6 shows the average measured shear wave velocities of samples with the same void ratios at the confining effective stress of 100 kPa along with the liquefaction curves.

5.2. Small-strain shear modulus calculation

In the bender element test, shear waves propagate through the sample with induced maximum shear strain of less than 10^{-5}. Thus, having measured the V_s, the small-strain shear modulus can be obtained using Eq. (4). In this equation, G_0 is the small-strain shear modulus and ρ is the total density of the soil.

$$G_0 = \rho V_s^2 \tag{4}$$

For a granular soil, G_0 is a function of its void ratio and effective confining stress, and can be obtained from the empirical equation

Table 2
Intrinsic parameters of Eq. (5) for tested sands.

Sand type	C_g	n_g	a_g	R^2
Babolsar	449.7	0.453	−1.885	0.986
Firoozkooh	389.1	0.478	−1.835	0.955

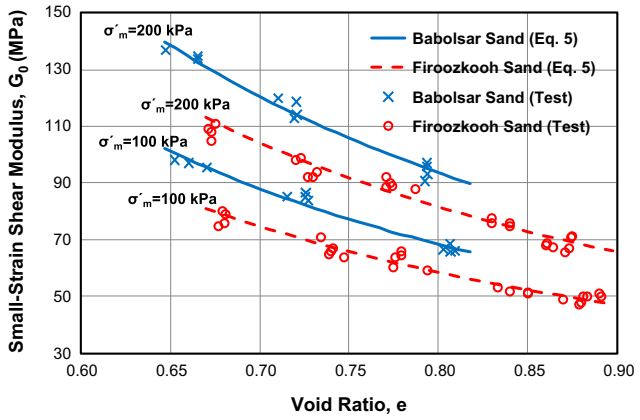

Fig. 10. Small-strain shear modulus versus void ratio for tested sands at different consolidation stresses.

like the one developed by Jamiolkowski et al. [33], as introduced in Eq. (5).

$$G_0 = C_g P_A^{1-n_g} e^{a_g} \sigma_m^{'n_g} \tag{5}$$

where P_A is the reference atmospheric pressure equal to 100 kPa, $\sigma_m^{'}$ is the mean effective stress in the same units as the reference stress and can be calculated using Eq. (6). The parameters a_g, n_g, and C_g are intrinsic parameters associated with each type of material.

$$\sigma_m^{'} = \frac{1+2K_0}{3}\sigma_v^{'} \tag{6}$$

In Eq. (6), $\sigma_v^{'}$ is the vertical effective stress and K_0 is the ratio of effective horizontal stress to effective vertical stress.

The intrinsic parameters of Eq. (5) for Firoozkooh and Babolsar sands were obtained by fitting the results of the all bender element tests conducted at different consolidation stresses and void ratios. These parameters are listed in Table 2. The table shows that the values of correlation coefficient, R^2, for both sand types are very close to 1.0, indicating that the correlation is satisfactory.

The small-strain shear modulus of Firoozkooh and Babolsar sands at 100 and 200 kPa consolidation stresses versus void ratio are illustrated in Fig. 10, using Eq. (5) and the corresponding intrinsic parameters for each sand type from Table 2. Obviously, similar curves can be drawn at other isotropic effective stresses. The data points of measured G_0 values at effective confining stresses of 100 and 200 kPa are also provided in Fig. 10. As expected, G_0 decreases with increasing void ratio and decreasing the confining effective stress.

6. CRR–V_s correlation

6.1. Establishment of the correlation

In this section, the detailed procedure for establishment of CRR–V_s correlation is presented. Both the cyclic resistance and the V_s values measured in the laboratory must be corrected to represent the field conditions. In a triaxial test, K_0 is equal to 1,

but for saturated normally consolidated sand in the field, K_0 is generally between 0.4 and 0.5. Also, seismic excitations in the field are multi-directional, while in a cyclic triaxial test, the cyclic load is applied in only one direction. Therefore, to account for these differences, the liquefaction resistance of the soil obtained from cyclic triaxial tests should be corrected. Several equations have been suggested in the literature regarding such corrections. In this study, the widely accepted equation proposed by Seed [34] was used in this respect as follow:

$$\mathrm{CRR} = 0.9\left(\frac{1+2K_0}{3}\right)\mathrm{CRR}_{\mathrm{tx-15\ cycles}} \tag{7}$$

where, CRR is the actual liquefaction resistance in the field, and the value of 0.9 is a factor to account for the strength loss occurring in the field during the multidirectional shaking in real earthquakes compared with unidirectional laboratory testing.

On the other hand, using Eqs. (5) and (6), the actual on-site small-strain shear modulus (G_{01}) can be modified by the following equation to consider the effects of K_0.

$$G_{01} = \left(\frac{1+2K_0}{3}\right)^{n_g} G_{01,\ \mathrm{tx}} \tag{8}$$

where G_{01} is the small-strain shear modulus at a vertical effective stress of 100 kPa in the field, and $G_{01,\ \mathrm{tx}}$ is the small-strain shear modulus obtained in the laboratory at an confining effective stress of 100 kPa ($=P_A$).

According to Eq. (5):

$$G_{01,\ \mathrm{tx}} = C_g P_A e^{a_g} \tag{9}$$

Combining Eqs. (2) and (7) leads to the following equation:

$$\mathrm{CRR} = 0.9\alpha e^{\beta}\left(\frac{1+2K_0}{3}\right) \tag{10}$$

Also combining Eqs. (8) and (9) the following equation is obtained:

$$G_{01} = C_g P_A e^{a_g}\left(\frac{1+2K_0}{3}\right)^{n_g} \tag{11}$$

Using Eqs. (10) and (11), by eliminating the void ratio (e), the correlation between the field small-strain shear modulus at vertical effective stress of 100 kPa (G_{01}) and the field liquefaction resistance (CRR) can be established (Eq. (12)). Using Eq. (4), also the correlation between CRR and V_{s1} (V_s at a vertical effective stress of 100 kPa) is obtained as follow:

$$\mathrm{CRR} = (K_c P_A^{-1} G_{01})^{n_c} = (K_c P_A^{-1}\rho V_{s1}^2)^{n_c} \tag{12}$$

In this equation, G_{01} and P_A are in the same units. All parameters in Eq. (12), except K_c and n_c have been defined previously. K_c and n_c are defined as

$$K_c = (0.9\alpha)^{a_g/\beta}\left(\frac{1}{C_g}\right)\left(\frac{1+2K_0}{3}\right)^{(a_g/\beta)-n_g} \tag{13}$$

$$n_c = \frac{\beta}{a_g} \tag{14}$$

Using Eq. (12) and having the required values of intrinsic parameters for G_0 (i.e. a_g, n_g and C_g) and coefficients relating the cyclic liquefaction resistance ratio to void ratio (i.e. α and β), the CRR–V_{s1} correlation can be obtained for any soil type. For Eq. (12), CSR=0.03 is also considered as the threshold of pore pressure generation [35].

In order to obtain the V_s at an effective vertical stress of 100 kPa in the field (V_{s1}), the measured in-situ shear wave velocity ($V_{s,\ \mathrm{field}}$) should be normalized with the effective overburden stress (σ'_v).

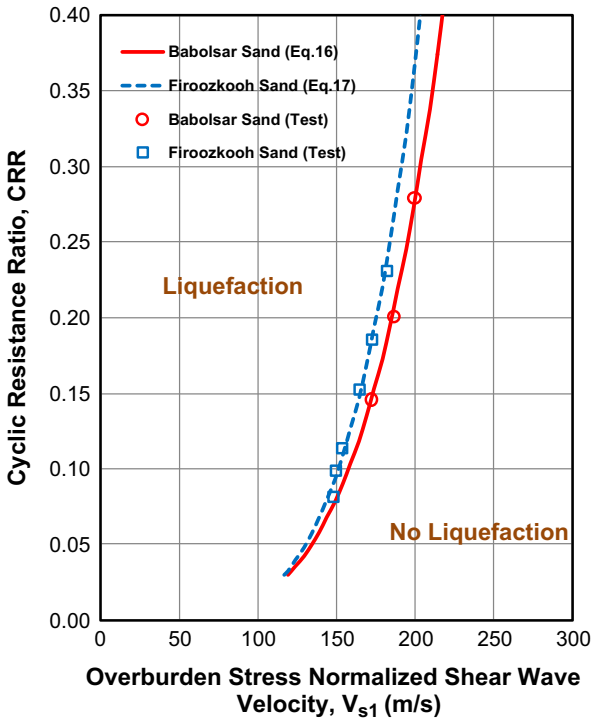

Fig. 11. CRR–V_{s1} correlation of tested sands.

The following equation can be used for this purpose.

$$V_{s1} = V_{s,\ \mathrm{field}}\left(\frac{P_A}{\sigma'_v}\right)^{0.25} \tag{15}$$

6.2. The CRR–V_{s1} correlation for tested sands

Substituting the parameters α and β from the cyclic triaxial tests (Fig. 7) and a_g, n_g, and C_g from the bender element tests (Table 2) in Eq. (12) and assuming K_0 to be 0.5, Eqs. (16) and (17) are derived to correlate CRR and V_{s1} values for Babolsar and Firoozkooh sands, respectively.

$$\mathrm{CRR} = (6.2\times 10^{-6}\rho V_{s1}^2)^{1.92} \tag{16}$$

$$\mathrm{CRR} = (7.6\times 10^{-6}\rho V_{s1}^2)^{2.07} \tag{17}$$

In these equations, V_s is expressed in m/s and the soil density is in g/cm^3. Although the grain size distribution curves for Babolsar and Firoozkooh sands are rather similar (Fig. 2), Eqs. (16) and (17) show that the correlation between V_s and liquefaction resistance for these two sands are different.

Using Eqs. (16) and (17), the predicted CRR–V_{s1} curves of tested sands are plotted in Fig. 11. The experimental data points from Fig. 6 which are modified by Eqs. (7) and (8) to represent the field conditions are also provided in this figure. Fig. 11 shows that there is a very good agreement between predicted CRR–V_{s1} correlation from Eq. (12) and the experimental results. It can be concluded that the suggested equation (Eq. (12)) can be used to develop the soil-specific CRR–V_{s1} correlations.

6.3. CRR–V_{s1} correlation for other sands

In this study, comprehensive investigations in the literature were performed to obtain similar laboratory data for six other sands. The physical properties of these sands are listed in Table 3. Compiling the experimental data obtained from the literature for these six types of sands on reconstituted specimens, the

Table 3
Intrinsic parameters and physical properties of some clean sands along with the relevant references.

Sand type	Physical properties					Liquefaction resistance parameters[b]				Intrinsic parameters for small-strain shear modulus evaluation			
	D_{50}	C_u	e_{max}	e_{min}	G_s	α	β	R^2	Ref.	C_g	n_g	a_g	Ref.
Toyoura	0.21	1.6	0.972	0.609	2.65	0.059	−4.187	0.991	[36]	724	0.45	−1.3	[37]
Niigata	N.A.	1.8	1.230	0.770	2.69	0.100	−6.469	0.980	[4]	360[b]	0.5[a]	−2.336[b]	[4]
Mai Liao	N.A.	N.A.	1.125	0.646	2.69	0.165	−3.951	0.966	[22]	415[b]	0.5[a]	−1.567[b]	[22]
Monterey	0.43	1.5	0.821	0.631	2.65	0.088	−3.515	0.908	[38]	477[b]	0.5[a]	−1.04[b]	[13]
Fuzhou	0.34	3.0	0.790	0.430	2.65	0.007	−5.706	0.972	[19]	408[b]	0.493[b]	−1.108[b]	[19]
Ottawa	0.38	1.4	0.780	0.480	2.65	0.024	−4.559	0.979	[39]	364[b]	0.534[b]	−2.07[b]	[40]

Note: [a]Assumed, [b]Calculated by fitting the provided data and N.A. Not available.

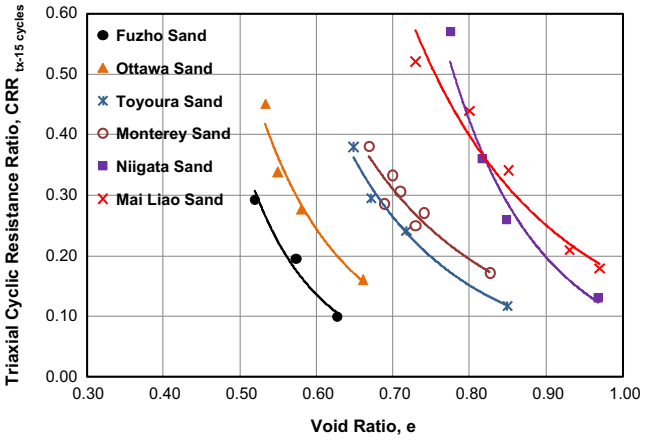

Fig. 12. $CRR_{tx\text{-}15\ cycles}$ versus void ratio for different sand types.

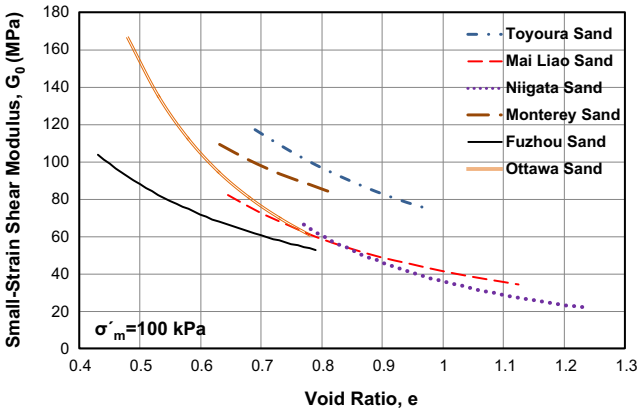

Fig. 13. Small-strain shear modulus versus void ratio for different sands at a consolidation stress of 100 kPa.

liquefaction resistances at different void ratios were obtained accordingly. Triaxial liquefaction resistances versus void ratios for these sands are shown in Fig. 12. The corresponding values of α and β obtained by fitting appropriate power curves to the laboratory data together with the reference papers from which these data are obtained are provided in Table 3. The table shows that the values of R^2, for all sand types are close to 1.0 indicating that Eq. (2) is a good correlation between void ratio (e) and liquefaction resistance ($CRR_{tx\text{-}15\ cycles}$). For these sands, the values of intrinsic parameters of the G_0 correlation (i.e. a_g, n_g and C_g in Eq. (5)) were also calculated by fitting curves to the provided data from the literature which are also presented in Table 3. In cases where the parameter n_g was not provided, the value of n_g was considered to be 0.5 which have been shown to be a good approximation.

The small-strain shear modulus curves versus void ratio for these sand types at a consolidation stress of 100 kPa, using Eq. (5) and the provided intrinsic parameters in Table 3, are also presented in Fig. 13.

Finally, the CRR–V_{s1} correlations for these sands were obtained using the data presented in Table 3 and Eq. (12). Assuming K_0 to be 0.5, intrinsic parameters of Eq. (12) (K_c and n_c) for these sands together with those for the tested sands were calculated and are presented in Table 4.

It is shown that the power of V_{s1} in CRR–V_{s1} correlation (which is $2n_c$) for these sands ranges from 3.84 to 10.3. It is worth noting that according to the studies conducted by Chen et al. [18], the suggested power of V_{s1} is 4. Also Zhou and Chen [19] concluded that the power of V_{s1} is in the range of 1.8 to 6. Noteworthy is that further studies are required to investigate the effects of different soil parameters on intrinsic parameters for CRR–V_{s1} correlation (i.e. K_c and n_c). This is considered to be beyond the scope of this study.

Using the data in Table 4 and Eq. (12), the CRR–V_{s1} curves for these six types of sands together with two tested sands are shown in Fig. 14. It is noteworthy that the variations of G_0 or CRR with void ratio (e) and confining stresses are characterized by Eqs. (2) and (5) respectively. Since Eq. (12) is based on these two equations, it is possible to extrapolate somewhat the CRR–V_{s1} correlation beyond the limits of the performed tests using this equation. In Fig. 14, to indicate the extrapolation parts of the CRR–V_{s1} curves beyond the tested range, these parts of curves are shown with different style. As can be seen in Fig. 14, these curves are different for each type of sand. Therefore, it can be concluded that the CRR–V_{s1} correlation for these eight sand types is highly soil-specific. As a result, for an accurate assessment of liquefaction potential for a given sand type, it is required to determine a soil-specific CRR–V_{s1} correlation for that sand.

Table 4
Intrinsic parameters of CRR–V_{s1} correlation for different sands.

Sand type	K_c ($\times 10^{-4}$)	n_c
Babolsar	6.2	1.92
Firoozkooh	7.6	2.07
Toyoura	5.9	3.22
Niigata	12.3	2.77
Mai Liao	11.8	2.52
Monterey	7.6	3.38
Fuzhou	10.5	5.15
Ottawa	5.0	2.20

7. Discussion

7.1. Uniqueness of CRR–V_{s1} correlation

As previously mentioned, several researchers have proposed curves for evaluating liquefaction resistance through V_s measurements. Fig. 15

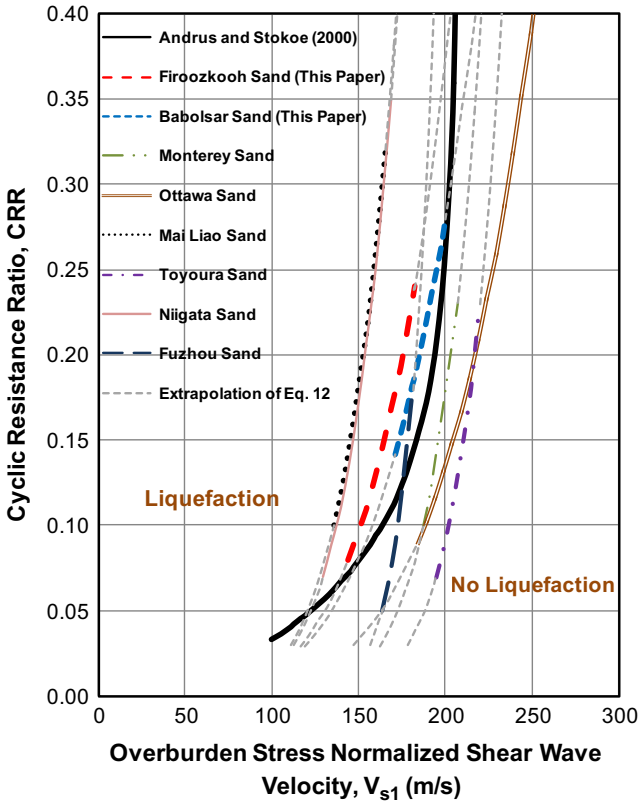

Fig. 14. Proposed laboratory-based correlations for different sands together with the existing field-based CRR–V_{s1} correlations of Andrus and Stokoe [2].

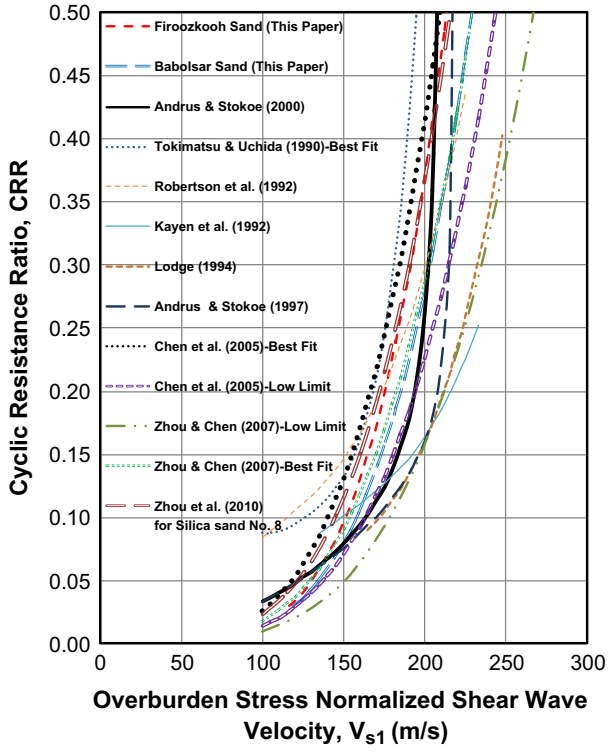

Fig. 15. Comparison between different proposed CRR–V_{s1} curves.

is a compilation of the most important CRR–V_{s1} curves proposed by different researchers for clean sandy soils and also those of Babolsar and Firoozkooh sands obtained in this study. Fig. 15 includes CRR–V_{s1} curves that have been developed based on field performance observations (i.e. proposed curves by Robertson et al. [15]; Kayen et al. [16]; Lodge [17]; and Andrus and Stokoe [24,2]) as well as those that have been developed based on laboratory tests (i.e. proposed curves by Tokimatsu and Uchida [4]; Chen et al. [18]; Zhou and Chen [19] and Zhou et al. [20]). The scattering of the curves in Fig. 15 suggest that the CRR–V_{s1} may not be unique. The different curves obtained for different sand types in the present study, including those that have been tested and those that have been compiled from the literature (Fig. 14) also confirm that there is not a unique CRR–V_{s1} curve for all types of sands.

7.2. Comparison with the existing procedure

As mentioned earlier in Section 1, Andrus and Stokoe [2] suggested a method for the evaluation of liquefaction potential based on field V_s measurements. This method is recommended by NCEER and is widely used in current practice. It follows the framework of the Seed–Idriss simplified procedure [1], correlating the overburden stress-corrected shear wave velocity (V_{s1}) to the magnitude-scaled cyclic stress ratio (CSR) induced by earthquakes. In this method, CRR is calculated from the following equation:

$$\mathrm{CRR} = \left\{ a\left(\frac{V_{s1}}{100}\right)^2 + b\left(\frac{1}{V_{s1}^* - V_{s1}} - \frac{1}{V_{s1}^*}\right) \right\} \tag{18}$$

where V_{s1}^* is the limiting upper value of V_{s1} for cyclic liquefaction occurrence with an assumed value of 215 m/s for clean sand; a and b are curve fitting parameters taken to be 0.022 and 2.8 respectively.

The CRR–V_s curve suggested by Andrus and Stokoe [2] are also plotted in Figs. 14 and 15. As can be seen, although this proposed method can be used as an initial estimation of liquefaction resistance, it may underestimate or overestimate the liquefaction resistance of different sandy soils. For a more accurate assessment of the liquefaction resistance of a sandy soil, a soil-specific CRR–V_{s1} correlation is needed.

7.3. The region for soil-specific CRR–V_{s1} curves

Using the CRR–V_{s1} curves developed by different researchers (Fig. 15) and also those obtained for eight different sands in this study (Fig. 14), a region can be determined in which all the CRR–V_{s1} curves are located. In Fig. 16, this region is defined as the region of "Suspected to liquefaction". All the soil-specific CRR–V_{s1} curves are most likely to be located in this region. Considering that all the curves presented in Figs. 14 and 15 are located within this region, the provided chart is based on field performance observations as well as the results of laboratory tests.

This region is bounded by two parallel lines. One line extending from the point of CRR=0 and V_{s1}=90 m/s to the point of CRR=0.5 and V_{s1}=180 m/s and the other line extending from the point of CRR=0 and V_{s1}=180 m/s to the point of CRR=0.5 and V_{s1}=270 m/s. Also as mentioned in Section 6.1, below CSR=0.03 soil is considered non-liquefiable.

7.4. Practical applications

For liquefaction assessment at a specific site, in addition to the resistance of the soil to liquefaction (CRR), obtained from the CRR–V_{s1} curves, the level of cyclic loading on the soil caused by the earthquake (CSR) should also be determined. Based on the simplified procedure, liquefaction may occur at points where CSR exceeds the CRR.

All the proposed curves for the estimation of CRR (Figs. 14–16) are for an earthquake moment magnitude of M_w=7.5. Therefore, the CRR derived from these curves would be scaled for other

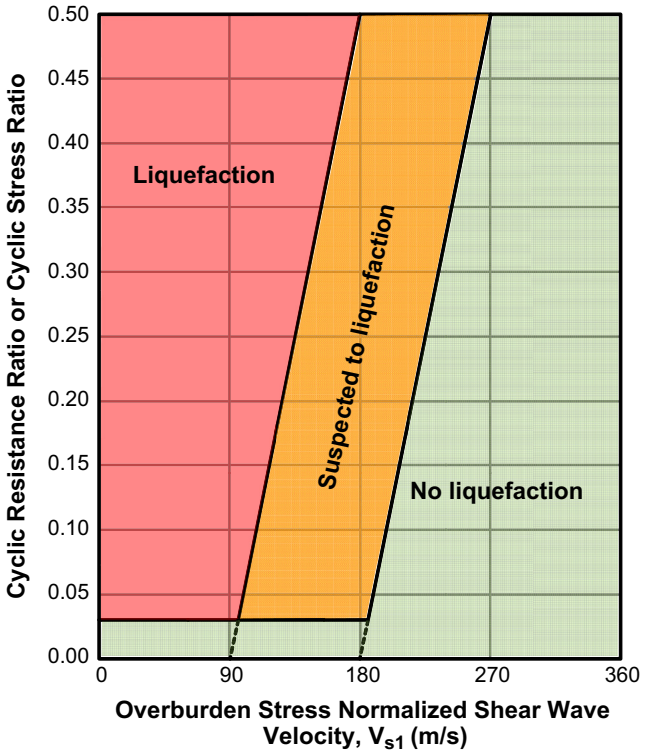

Fig. 16. Regions of "Liquefaction", "No liquefaction" and "Suspected to liquefaction".

earthquake magnitudes by applying a magnitude scaling factor (MSF). Instead of scaling the CRR parameter, another approach is to scale the CSR parameter for a specified earthquake (CSR_{M_w}) other than $M_w=7.5$ using Eq. (19) as below:

$$CSR = CSR_{M_w}/MSF \tag{19}$$

Corrections for consideration of other factors that affect the liquefaction resistance, e.g. effective overburden pressure, initial shear stresses, cementation and aging effects are applicable in the same manner.

The field measured value of V_s corrected to V_{s1} together with the scaled value of CSR for a specified earthquake at a specific location in a sandy soil layer define a point in Fig. 16. If this point falls within the region specified as "No liquefaction" in Fig. 16, then the liquefaction will not occur in that specific location for the specified earthquake. On the other hand, if the point falls within the region specified as "Liquefaction", then liquefaction will occur at that specific location due to the specified earthquake. In both cases described above, there is no need to establish the soil-specific CRR–V_{s1} correlation. However if the point falls within the region specified as "Suspected to liquefaction", then in order to determine if the soil in the specified location in that field is liquefiable or not by the specified earthquake, it is necessary to obtain the soil-specific CRR–V_{s1} correlation for the soil of that field. In case, the soil-specific CRR–V_{s1} correlation cannot be established, that specific location may be considered to liquefy for the given earthquake. In other words, to be conservative in such a case, the line drawn from the point of CRR=0 and $V_{s1}=180$ m/s to the point of CRR=0.5 and $V_{s1}=270$ m/s can be considered as the boundary line between liquefiable and non-liquefiable soil conditions.

Therefore, for the liquefaction potential microzonation using V_s measurements, the mapped area can be classified as one of these three different zones: 1 – liquefiable zone, 2 – non-liquefiable zone, and 3 – zone with liquefaction susceptibility.

It is worth noting that for a zone with liquefaction susceptibility, one of these two approaches can be used: (1) preparation of soil-specific CRR–V_{s1} curve or (2) adopting a conservative approach, and considering the zone to be liquefiable. The choice of one of these approaches can also be based on economic aspect of the project at hand.

8. Summary and conclusion

In this paper, a new semi-empirical equation is suggested to correlate the cyclic resistance ratio (CRR) and the overburden stress-corrected shear wave velocity (V_{s1}) values from laboratory tests data.

Laboratory measurements of V_s using bender element tests and the liquefaction resistance estimation using cyclic triaxial tests were performed on two types of clean sands, namely Firoozkooh and Babolsar sands. Using the proposed method, the soil-specific CRR–V_{s1} correlations were established for these two sands.

In addition, the laboratory test data for six other sands gathered from the literature, were compiled to obtain the soil-specific CRR–V_{s1} correlations for these sands.

The results of this study show that although there is a good correlation between shear V_s and liquefaction resistance, this correlation is not unique for different types of sandy soils and is soil-specific.

The accuracy of the widely used simplified method for evaluation of liquefaction potential from V_s measurements was also investigated. It was found that the simplified method, proposed by Andrus and Stokoe [2], can only be used as an initial estimation of liquefaction resistance. To accurately evaluate the liquefaction potential from V_s measurements, it may be necessary to develop the soil-specific CRR–V_{s1} correlations by laboratory tests. The method proposed in this paper can be used for development of such soil-specific correlations from laboratory tests.

Using the CRR–V_{s1} curves obtained for eight different sands in this study and the curves suggested by other investigators which are based on field performance observations or laboratory tests, a region is introduced in which all the soil-specific CRR–V_{s1} curves are likely to be located. Therefore, for practical use, by measuring the field V_s in a specified area and using the proposed chart, for a given earthquake, the investigated area can be classified into three different zones: 1 – liquefiable zone, 2 – non-liquefiable zone, and 3 – zone with liquefaction susceptibility. The soil-specific CRR–V_{s1} correlation will not be required in zones with liquefaction potential and zones with no liquefaction potential. But in the suspected to liquefaction potential zones, if the accurate assessment of liquefaction potential is desired, the soil-specific CRR–V_{s1} correlation will be required; otherwise, as a conservative approach, this zone may be considered to have liquefaction potential.

References

[1] Seed HB, Idriss IM. Simplified procedure for evaluating soil liquefaction potential. J Geotech Eng Div ASCE 1971;97(9):1249–73.
[2] Andrus RD, Stokoe II KH. Liquefaction resistance of soils from shear wave velocity. J Geotech Geoenviron Eng 2000;126(11):1015–25.
[3] Baxter CDP, Bradshaw AS, Green RA, Wang J. Correlation between cyclic resistance and shear-wave velocity for providence silts. J Geotech Geoenviron Eng 2008;134(1):37–46.
[4] Tokimatsu K, Uchida A. Correlation between liquefaction resistance and shear wave velocity. Soils Found 1990;30(2):33–42.
[5] De Alba P, Baldwin K, Janoo V, Roe G, Celikkol B. Elastic-wave velocities and liquefaction potential. Geotech Test J 1984;7(2):77–87.
[6] Yoshimi Y, Tokimatsu K, Kaneko O, Makihara Y. Undrained cyclic shear strength of a dense Niigata sand. Soils Found 1984;24(4):131–45.
[7] Wang JH, Moran K, Baxter CDP. Correlation between cyclic resistance ratios of intact and reconstituted offshore saturated sands and silts with the same shear wave velocity. J Geotech Geoenviron Eng 2006;132(12):1574–80.
[8] Leon E, Gassam SL, Talwani P. Accounting for soil aging when assessing liquefaction resistance. J Geotech Geoenviron Eng 2006;132(3):363–77.
[9] U.S. Bureau of Reclamation (USBR). Seismic design and analysis. Chapter 13. Design standards no. 13. Embankment Dams, Denver, CO; 1989. p. 28–9.

[10] Boulanger RW, Mejia LH, Idriss IM. Liquefaction at moss landing during Loma Prieta earthquake. J Geotech Geoenviron Eng 1997;123(5):453–67.
[11] Roy D, Campanella RG, Byrne PM, Hughes JMO. Strain level and uncertainty of liquefaction related index tests. In: Shackelford CD, Nelson PP, Roth MJS, editors. Uncertainty in the geologic environment: from theory to practice Geotech Spec Publ No.58, vol. 2. New York: ASCE; 1996. p. 1149–62.
[12] Liu N, Mitchell JK. Influence of nonplastic fines on shear wave velocity-based assessment of liquefaction. J Geotech Geoenviron Eng 2006;132(8):1091–7.
[13] Salgado R, Bandini P, Karim A. Shear strength and stiffness of silty sand. J Geotech Geoenviron Eng 2000;126(5):451–62.
[14] Tokimatsu K, Yamazaki T, Yoshimi Y. Soil liquefaction evaluation by elastic shear moduli. Soils Found 1986;26(1):25–35.
[15] Robertson PK, Woeller DJ, Finn WDL. Seismic cone penetration test for evaluating liquefaction potential under cyclic loading. Can Geotech J 1992;29:686–95.
[16] Kayen RE, Mitchell JK, Seed RB, Lodge A, Nishio S, Coutinho RQ. Evaluation of SPT-, CPT-, and shear wave-based methods for liquefaction potential assessments using Loma Prieta data. In: Proceedings of the 4th US–Japan workshop on earthquake resistant design of lifeline facilities and countermeasures for soil liquefaction, NCEER-92-0019. National Center for Earthquake Engineering Research, Buffalo, N.Y.; 1992. p. 177–92.
[17] Lodge AL. Shear wave velocity measurements for subsurface characterization. Phd dissertation. Berkeley, CA: University of California; 1994.
[18] Chen YM, Ke H, Chen RP. Correlation of shear wave velocity with liquefaction resistance based on laboratory tests. J Soil Dyn Earthq Eng 2005;25(6):461–9.
[19] Zhou YG, Chen YM. Laboratory investigation on assessing liquefaction resistance of sandy soils by shear wave velocity. J Geotech Geoenviron Eng 2007;133(8):959–72.
[20] Zhou YG, Chen YM, Shamoto Y. Verification of the soil-type specific correlation between liquefaction resistance and shear-wave velocity of sand by dynamic centrifuge test. J Geotech Geoenviron Eng 2010;136(1):165–77.
[21] Dobry R, Stokoe II KH, Ladd RS, Youd TL. Liquefaction susceptibility from S-wave velocity. In: Proceedings of ASCE national convention, in situ tests to evaluate liquefaction susceptibility. New York: ASCE; 1981.
[22] Huang YT, Huang AB, Kuo YC, Tsai MD. A laboratory study on the undrained strength of a silty sand from Central Western Taiwan. J Soil Dyn Earthq Eng 2004;24:733–43.
[23] Stokoe II KH, Nazarian S. Use of Rayleigh waves in liquefaction studies. In: Proceedings of the measurement and use of shear wave velocity for evaluating dynamic soil properties. ASCE: New York, N.Y.; 1985. p. 1–17.
[24] Andrus RD, Stokoe II KH. Liquefaction resistance based on shear wave velocity. In: Youd TL, Idriss IM, editors. Proceedings of the NCEER workshop on evaluation of liquefaction resistance of soils, Tech. Rep. NCEER-97-0022. Buffalo: National Center for Earthquake Engineering Research; 1997. p. 89–128.
[25] Bierschwale JG, Stokoe II KH. Analytical evaluation of liquefaction potential of sands subjected to the 1981 Westmorland earthquake. Geotechnical Engineering Report. GR-84-15; 1984.
[26] Kayen RE, Seed RB, Moss RE, Cetin O, Tanaka Y, Tokimatsu K. Global shear wave velocity database for probabilistic assessment of the initiation of seismic-soil liquefaction. In: Proceedings of the 11th international conference on soil dynamics and earthquake engineering, vol. 2. Berkeley: University of California and Stallion Press; 2004. p. 506–12.
[27] Juang CH, Jiang T, Andrus RD. Assessing probability-based methods for liquefaction potential evaluation. J Geotechn Geoenviron Eng 2002;128(7):580–9.
[28] Ishihara K. Liquefaction and flow failure during earthquakes. Geotechnique 1993;43(3):351–415.
[29] Ladd RS. Preparing test specimens using undercompcation. Geotech Test. J ASTM 1978;1(1):16–23.
[30] Boulanger RW. High overburden stress effects in liquefaction analyses. J Geotech Geoenviron Eng 2003;129(12):1071–82.
[31] Lee JS, Santamarina JC. Bender elements: performance and signal interpretation. J Geotech Geoenviron Eng 2005;131(9):1063–70.
[32] Kumar J, Madhusudhan BN. A note on the measurement of travel times using bender and extender elements. J Soil Dyn Earthq Eng 2010;30(7):630–4.
[33] Jamiolkowski M, Leroueil S, Lo Presti DCF. Theme lecture: design parameters from theory to practice. In: Proceedings of Geo-Coast '91, Yokohama 1991;2:877–917.
[34] Seed HB. Soil liquefaction and cyclic mobility evaluation for level ground during earthquakes. J Geotech Eng Div, ASCE 1979;105(GT2)201–55.
[35] Dobry R, Ladd R, Yokel F, Chung R, Powell D. Prediction of pore water pressure buildup and liquefaction of sands during earthquakes by the cyclic strain method. National bureau of standards building science series. US Department of Commerce; 1982. p. 138.
[36] Oda M, Kawamoto K, Suzuki K, Fujimori H, Sato M. Microstructural interpretation on reliquefaction of saturated granular soils under cyclic loading. J Geotech Geoenviron Eng 2001;127(5):416–23.
[37] Lo Presti DCF, Jamiolkowski M, Pallara O, Cavallaro A, Pedroni S. Shear modulus and damping of soils. Geotechnique 1997;47(3):603–17.
[38] Polito PC, Martin JrII. Effect of nonplastic fines on the liquefaction resistance of sands. J Geotech Geoenviron Eng 2001;127(5):408–15.
[39] Carraro JAH, Bandini P, Salgado R. Liquefaction resistance of clean and nonplastic silty sands based on cone penetration resistance. J Geotech Geoenviron Eng 2003;129(11):965–76.
[40] Robertson PK, Sasitharan S, Cunning JC, Sego DC. Shear-wave velocity to evaluate in-situ state of Ottawa sand. J Geotech Eng 1995;121(3):262–73.